

# LOVE WAVE AND LAYER GUIDED SHEAR HORIZONTAL ACOUSTIC PLATE MODE SENSORS

G McHale      The Nottingham Trent University, Department of Chemistry and Physics, Clifton Lane,  
Nottingham NG11 8NS, UK  
M I Newton    The Nottingham Trent University, Department of Chemistry and Physics, Clifton Lane,  
Nottingham NG11 8NS, UK

## 1. INTRODUCTION

This paper describes some key results on the mass sensitivity of layer guided acoustic waves arising from recent research at Nottingham Trent University into the use of Love waves for biosensing. More than thirty years ago it was suggested that surface acoustic waves (SAWs) could be excited by an interdigital transducer. Subsequent progress on the use of SAW devices as RF filters in telecommunications applications was rapid and current technology has enabled a range of devices, including high Q resonators working well into the GHz range. In such applications, care is taken to ensure the state of the device surface does not change as the acoustic wave is highly sensitive to surface mass loading. Over the last twenty years this mass sensitivity has been exploited to create a range of gas/vapour phase sensors. The most commonly used mode is the Rayleigh-SAW, which has a mechanical component of displacement perpendicular to the surface. Over the last decade the use of acoustic wave devices as sensors has been extended to the liquid phase and to mass deposition from the liquid phase. This has presented new challenges because any displacement perpendicular to the device surface may, under appropriate conditions, generate compressional waves in the adjacent liquid that give rise to excessive attenuation. Two approaches can be taken to obviate the compressional wave difficulty. The first approach is to use a flexural plate wave (FPW) which, although it has a surface perpendicular component, also has a speed of propagation less than the speed of sound in the liquid. The second approach is to use an acoustic wave mode that has only in-plane displacements. A range of such shear modes have been used for liquid phase sensing.

The simplest shear mode acoustic wave sensor is the quartz crystal microbalance (QCM). This uses a thickness shear mode of vibration. In the gas phase the face of the crystal is sensitive to any deposited mass and when incorporated into a resonator circuit the downward shift in resonant frequency is proportional to product of the mass per unit area and the square of the frequency. However, when one face of the quartz crystal is placed in contact with a liquid, such as water, the shear vibrations of the surface couple in a damped shear wave in the liquid. The penetration depth of this shear wave depends on the inverse square root of the frequency and the QCM effectively measures the mass of liquid within an interfacial layer. In a liquid, the downward shift in the frequency of the QCM depends on the product of the square root of the viscosity-density product and the frequency to a reduced power of  $3/2$ . In the liquid phase, the QCM also retains its vapour phase ability of being able to detect mass deposited from the liquid. Unfortunately, biosensing applications require higher mass sensitivity than is provided by QCM's operating at their usual frequencies of 5-10 MHz. Increasing their sensitivity by increasing frequency becomes untenable because this requires ever thinner crystals which thus become fragile. Interest in acoustic wave modes has therefore focused on alternative surface acoustic wave type modes as these do not require thin substrates. The most obvious alternatives are to use a substrate and a propagation axis supporting either a shear horizontal surface acoustic wave (SH-SAW) or a shear horizontal acoustic plate mode (SH-APM). Both of these modes have been used for sensing the liquid viscosity-density product. However, these devices have not possessed sufficient sensitivity for biosensing applications and, hence, much effort has focused on the use of SH-SAW type devices involving some element of waveguiding. The rationale behind this has been to localise the wave to the surface and so maximise the displacement of the surface to which mass attaches from the liquid phase. One wave-guiding technique uses a set of metallized bars in the propagation path to create a surface transverse wave (STW) mode. An alternative, which we have studied, uses a wave-guiding layer possessing a lower shear acoustic speed than the substrate to create a device known as a Love wave.

## 2. LOVE WAVE AND SH-APM SENSORS

### 2.1 COMPARISON OF MODES

Love waves were first reported for use in biosensors in 1992 by Gizeli *et al* and by Kovacs and Venema and are currently believed to offer one of the highest potential mass sensitivities of acoustic wave devices. A Love wave is a shear horizontally polarised surface acoustic wave that is localised to the surface of a semi-infinite half space and guided by a layer which has a shear acoustic speed less than that of the half space material. The phase velocity of the Love wave is intermediate between that of the substrate and the layer and is determined by the layer thickness. In our work, the guiding layer is typically a polymer, such as poly(methylmethacrylate) or a photoresist, and the substrate is ST-quartz chosen such that the basic mode without a guiding layer is a surface skimming bulk wave (SSBW). Traditional Love waves are supported by a semi-infinite substrate and the displacement decays rapidly with depth. They have generally been regarded as distinct from shear horizontal acoustic plate modes (SH-APMs) whereby the substrate is finite and in which the substrate thickness determines a resonance. The lowest order,  $n=0$ , SH-APM mode corresponds to a plane wave whilst higher order SH-APM modes correspond to resonances of the substrate plate. Prior to our work the possibility of enhancing the mass sensitivity of SH-APM sensors by using a guiding layer, in a manner similar to Love waves, has not been considered. This seems peculiar since many features of the two sensors, as operated in practice, are similar (Figures 1a and 1b). Both use finite substrates, a shear horizontally polarised displacement and propagation in a delay line configuration between two sets of interdigital transducers (IDTs). In operation as mass sensors, both will have a mass layer, whether it is the wave-guiding layer or the mass layer being sensed. The major difference appears to be whether the displacement decays with depth into the substrate or whether the substrate acts as a resonator. Superficially this may appear to be a major difference, but in detail it is little more than a change in the boundary condition at the lower surface of the substrate. Moreover, we would anticipate that a crossover from a system with a resonating substrate to one with the decay condition should be possible within a single unified theoretical model. Therefore, a physical understanding of the spectrum of shear horizontally polarised acoustic modes occurring in a Love wave configuration on a finite substrate is of interest.

### 2.2 DISPERSION CURVES

The problem of the response of a two-layer system of a substrate and a wave-guide to the deposition of rigid mass is essentially the problem of the propagation of shear horizontal acoustic waves in a three-layer system. For the finite substrate Love wave and layer guided SH-APM sensors, we consider a substrate of thickness,  $w$ , with a density  $\rho_s$  and Lamé constants  $\lambda_s$  and  $\mu_s$  overlayed by a uniform mass layer of thickness,  $d$ , and with a density  $\rho_l$  and Lamé constants  $\lambda_l$  and  $\mu_l$ . In analogy to Love wave theory, the uniform mass overlayer is referred to as the guiding layer; this two-layer system is the bare sensor and possesses a dispersion curve. The third layer has a thickness,  $h$ , with a density  $\rho_p$  and Lamé constants  $\lambda_p$  and  $\mu_p$  and is referred to as a perturbing mass layer although the theory is not limited to a thin third layer. To derive a dispersion equation, wave motion in an isotropic and non-piezoelectric material of density  $\rho$  and with Lamé constants  $\lambda$  and  $\mu$  is considered. The displacements,  $u_j$  are then described by the equation of motion,

$$\rho \frac{\partial^2 u_j}{\partial t^2} = (\lambda + \mu) \frac{\partial S_{jj}}{\partial x_j} + \mu \nabla^2 u_j \quad (1)$$

and boundary conditions are applied to each of the interfaces. The solutions of the equation of motion are chosen to have a propagation along the  $x_1$  axis with displacements in the  $x_2$  direction of the sagittal plane ( $x_2, x_3$ ). They must also satisfy the boundary conditions on the displacements  $\underline{u}$  and the  $T_{13}$  component of the stress tensors. These must both be continuous at the interfaces between the substrate and guiding layer, and between the guiding layer and perturbing mass layer. The  $T_{13}$  component of the stress tensors must also vanish at the free surfaces of the substrate and the perturbing mass layer at  $x_3 = -w$  and  $x_3 = (d+h)$ , respectively. Using this approach we find the dispersion equation,

$$\tan(T_1 d) = \xi \tanh(T_s w) - \xi_p \tan(T_p h) [1 + \xi \tan(T_1 d) \tanh(T_s w)] \quad (2)$$

where the defining equations for the wave vectors  $T_s$ ,  $T_l$ , and  $T_p$ , are

$$T_s^2 = \omega^2 \left( \frac{1}{v^2} - \frac{1}{v_s^2} \right), \quad T_l^2 = \omega^2 \left( \frac{1}{v_l^2} - \frac{1}{v^2} \right), \quad T_p^2 = \omega^2 \left( \frac{1}{v_p^2} - \frac{1}{v^2} \right) \quad (3)$$

and the intrinsic speed of the layers are given by  $v_s = (\mu_s/\rho_s)^{1/2}$ ,  $v_l = (\mu_l/\rho_l)^{1/2}$  and  $v_p = (\mu_p/\rho_p)^{1/2}$ . The  $\xi$  and  $\xi_p$  have been defined as,

$$\xi = \frac{\mu_s T_s}{\mu_l T_l} \quad \text{and} \quad \xi_p = \frac{\mu_p T_p}{\mu_l T_l} \quad (4)$$

The second term on the right hand side of Eq. (2), which involves  $\xi_p \tan(T_p h)$ , is due to the presence of the third, perturbing, mass layer. Setting the thickness,  $h$ , of the perturbing mass layer to zero recovers the dispersion equation for the two-layer system of a substrate with a guiding layer. When the substrate thickness  $w \rightarrow \infty$  with  $T_s$  real, so that the  $\tanh(T_s w) \rightarrow 1$ , Eq. (2) gives the limit of a traditional Love wave perturbed by an arbitrary thickness perturbing mass layer; the Love wave solutions have  $v < v_s$ . Setting both the wave-guiding layer and perturbing layer thickness to zero and taking  $T_s = jk_s$ , where  $k_s$  is real, gives rise to the traditional SH-APM solutions which have  $v > v_s$ . Interestingly, setting the third layer thickness to zero and taking  $T_s = jk_s$ , where  $k_s$  is real, but retaining a finite thickness wave-guiding layer it is possible to obtain solutions with  $v > v_s$ , thus indicating that layer guided SH-APMs can exist.

It is possible to provide some analytical results for the acoustic wave modes in the two-layer system of finite thickness substrate and finite thickness wave-guiding layer. The thickness of the substrate,  $w$ , determines the number of Love wave modes and the spacing of the associated acoustic plate modes. At the start of each successive Love wave mode the phase speed of the Love wave is  $v = v_s$  and the speeds of the associated plate modes are  $v_m = v_s / (1 - (m\pi v_s / w\omega)^2)^{1/2}$  where  $\omega$  is the angular frequency. The thickness,  $d_{nm}$ , at which a new mode appears is,

$$\frac{d_{nm}}{\lambda_l} = \frac{n}{2 \sqrt{1 - \left( \frac{v_l}{v_s} \right)^2 \left[ 1 - \left( \frac{m\lambda_s}{2w} \right)^2 \right]}} \quad (5)$$

where  $n=0,1,2,3, \dots$  labels the successive Love wave modes and  $m=1,2,3, \dots$  labels the acoustic plate modes associated with each Love wave mode. Traditional Love waves correspond to  $m=0$  whilst acoustic plate modes correspond to  $m>0$ . The  $n=0$  Love wave corresponds to a displacement with a single node located within the substrate and an antinode at the surface of the guiding layer. Each higher order Love wave introduces an additional node within the layered system. Increasing the thickness of the guiding layer by an amount insufficient to change modes causes a reduction in the phase speed of the mode. Although it is not possible to analytically solve the dispersion equation, we have obtained the fractional change in phase speed caused by increasing the thickness of the guiding layer by an amount,  $\Delta d$ , above the guiding layer thickness resulting in the start of a mode. In the case of a Love wave  $\Delta v/v_s \propto \omega^2 \Delta d^2$ , assuming the substrate is sufficiently thick compared to the perturbation, whereas for the lower order associated acoustic plate modes we find  $\Delta v/v_s \propto \Delta d/w$ .

Numerical results for the phase speed obtained from the dispersion equation for the two-layer system using parameters of  $w=100 \mu\text{m}$ ,  $f=100 \text{ MHz}$ ,  $v_l=1100 \text{ ms}^{-1}$ ,  $v_s=5100 \text{ ms}^{-1}$ ,  $\rho_l=1000 \text{ kgm}^{-3}$  and  $\rho_s=2655 \text{ kgm}^{-3}$  are given in Figure 2. The horizontal-axis has been plotted using a dimensionless parameter of the wave-guiding layer thickness scaled by  $\lambda_l = v_l/f$ . With the exception of the substrate thickness, these parameters describe high frequency Love waves using a poly(methylmethacrylate) guiding layer on quartz. The substrate thickness in the calculation is thinner than typical substrates used in experiments, but this is solely to enable the acoustic plate modes to be resolved in Figure 2. The points shown in Figure 2 are the start of each mode calculated using the analytical results. Numerically, it is clear that each higher order Love wave mode, labelled by  $n=N$  and  $m=0$ , arises as a continuation of the acoustic plate mode, labelled by  $n=N-1$  and  $m=1$ , associated with the previous Love wave mode. This has been confirmed by computing the displacement functions. The form of the dispersion curve also suggests the intriguing possibility that the sensitivity of a SH-APM sensor can be significantly enhanced by the use of a wave-guide layer. The mass sensitivity of a Love wave device arises from the sharp change in phase speed,  $v$ , from a value equal to  $v_s$  to a value close to  $v_l$  that occurs at a wave-guiding layer thickness  $d \sim$

$(2n+1)\lambda_l/4$ , where  $n$  is the integer labelling the Love wave mode. In a Love wave sensor the wave-guiding layer thickness is usually chosen to place the device operating point at the transition point,  $d \sim \lambda_l/4$ , of the first Love wave mode. Any perturbation of this wave-guiding mass layer then causes the maximum change in phase speed. In a similar manner, we would expect that by using an SH-APM sensor with a wave-guide layer chosen to place the device operating point at the transition point,  $d \sim \lambda_l/4$ , a significantly enhanced mass sensitivity, compared to a device with no wave-guiding layer, could be obtained.

## 2.3 MASS SENSITIVITY

The effect of mass deposition on a Love wave or layer guided SH-APM sensor can be found from the dispersion equation for the three-layer system, Eq. (2), by perturbing about the solution for the two-layer system. Defining the combination,  $\rho_p h$ , of the density and thickness of the perturbing mass layer gives the mass per unit surface area,  $\Delta m$ , and this allows the fractional change in phase speed, from the speed,  $v_o$ , at the operating point of the dispersion curve, to be derived as,

$$\frac{\Delta v}{v_o} \approx \left(1 - \frac{v_p^2}{v_o^2}\right) g(\omega, v_s, \rho_l, v_l, w, d) \Delta m \quad (6)$$

where the function  $g$ , is known analytically and depends only upon the substrate, guiding layer and operating frequency. Experimentally, the significance of Eq. (6) is that if we can determine the sensitivity function,  $g$ , for any perturbing layer, then it is the same function for any other perturbing mass layer. The simplest case is to consider a small extension of the wave-guiding layer as the perturbing mass layer and this immediately leads to the conclusion that the sensitivity is intrinsically related to the slope of the dispersion curve. Defining a mass sensitivity function,  $S_m$ , we find,

$$S_m = \lim_{\Delta m \rightarrow 0} \frac{1}{\Delta m} \left( \frac{\Delta v}{v_o} \right) = \frac{1}{\rho_l} \left[ \frac{1 - v_p^2/v_o^2}{1 - v_l^2/v_o^2} \right] \left( \frac{d \log_e v}{dx} \right)_{x=d} \quad (7)$$

where the mass sensitivity function,  $S_m$ , is in units of  $\text{m}^2 \text{kg}^{-1}$ . Thus, the mass sensitivity of a Love wave or a layer-guided shear horizontally polarised acoustic plate mode device can be determined numerically from the experimentally or numerically determined dispersion curve. Figure 3 shows the modulus of the mass sensitivity,  $|S_m|$ , calculated from Eq. (7) for the first three Love wave modes in Figure 2. The corresponding curves for the layer-guided SH-APM modes are shown in Figure 4. As anticipated the maximum sensitivity occurs on the back-slope of each mode in Figure 2 which, for the parameter values used for the calculations, is at a guiding layer thickness of  $d \sim (2n+1)\lambda_l/4$ . Evaluating the analytical results for the mass sensitivities of non-layer guided SH-APM sensors gives  $|S_m| = 3.85, 4.92$  and  $8.91 \text{ m}^2 \text{kg}^{-1}$ , respectively, for the three  $m > 0$  SH-APM modes and these are in agreement with the numerical values in Figure 4 in the limit  $d \rightarrow 0$ . From Figure 4 it can be seen that the effect of the guiding layer on the SH-APM device is to dramatically increase the mass sensitivity by more than an order of magnitude. The greatest gain in mass sensitivity is with the highest order SH-APM mode. For the calculations in Figure 2 the mass sensitivity of the layer-guided SH-APMs becomes comparable to, to within an order of magnitude, the mass sensitivity of the Love wave modes. SH-APM devices have been increasingly discounted for biosensing applications due to their poorer sensitivity compared to Love wave devices. However, Love wave devices suffer from the problem of requiring the generating and receiving IDTs to be on the same face of the substrate as used for sensing. This causes problems due to the need for liquid seals in the propagation path and the potential coupling of electric fields via the liquid. SH-APM sensors use a resonance of both substrate faces and the mode can therefore be excited using IDTs placed on the back face of the substrate rather than the front face which has the layer in contact with the liquid. Thus, using a wave-guiding layer on an SH-APM to create a mass sensitivity comparable to Love wave devices whilst retaining the ability to excite the mode using the back face may be of great significance.

## 3. FREQUENCY DEPENDENCE OF LOVE WAVE SENSITIVITY

### 3.1 SENSITIVITY ON SEMI-INFINITE SUBSTRATE

In QCM sensors, for a uniform layer of mass the frequency dependence of the sensitivity function  $S_m$  is proportional to the frequency whilst for Newtonian liquids, such as water, it is proportional to the square root of frequency. Thus, a general guideline that arises for QCM sensors is that higher frequency provides greater sensitivity. For Love wave devices it is more difficult to give such simple general rules because the frequency dependence will depend on the chosen operating point on the dispersion curve. However, some key conclusions can be derived by considering a Love wave system with an infinite thickness substrate. In the case of a finite thickness substrate and finite thickness wave-guiding layer, the frequency enters the calculation of the wave-speed,  $v$ , through the two dimensionless combinations  $d/\lambda_l = dff/v_l$  and  $w/\lambda_s = wff/v_s$ . When the substrate is infinitely thick the layer guided SH-APMs are no longer possible and only Love waves can exist. Moreover, the phase speed for a Love wave then depends on frequency only through the dimensionless combination of  $z = d/\lambda_l = dff/v_l$ . This has important consequences for the mass sensitivity because a change in guiding-layer thickness,  $d$ , is then equivalent to a change in operating frequency,  $f$ . Thus, Eq. (7) can be used to assess the change in sensitivity that will occur through a change in operating frequency, for a given mass perturbation,  $\Delta m$ , on a particular device. The dispersion curve can be plotted using the dimensionless variable,  $z$ , and the slope on this dispersion curve can be related to the slope in the dispersion curve when plotted against guiding layer thickness. In dimensionless units of guiding layer thickness, the mass sensitivity function, Eq. (7), becomes,

$$S_m = \frac{1}{\rho_l} \left[ \frac{1 - v_p^2/v_o^2}{1 - v_l^2/v_o^2} \right] \frac{f_o}{v_l} \left( \frac{d \log_s v}{dz} \right)_{z=z_o} \quad (8)$$

and for perturbing materials with  $v_p \ll v_o$  this simplifies to,

$$S_m \approx \frac{1}{\rho_l} \frac{f_o}{v_l} \left( \frac{d \log_s v}{dz} \right)_{z=z_o} \quad (9)$$

### 3.2 FREQUENCY HOPPING

Experimentally, an increase in frequency may or may not be accompanied by a change in guiding layer thickness depending on how it is achieved. If the guiding layer thickness is not changed then the higher frequency may either move the operating point down the same Love wave mode or it may result in a change of mode. The consequences can be dramatically different with either a higher or lower mass sensitivity resulting from the increase in frequency depending on the slope of the dispersion curve at the new operating point. In Figure 5, the change indicated by a) which uses a change of  $z_o \rightarrow z_1$  due to increasing the frequency whilst retaining the same thickness guiding layer results in an increased sensitivity. However, the change indicated by b) which uses a change of  $z_1 \rightarrow z_2$ , due to increasing the frequency whilst retaining the same thickness guiding layer results in a decreased sensitivity. Both of these changes involve the device continuing to operate with a mode 1 Love wave. However, we have shown experimentally that for a polymer wave-guiding layer on ST-quartz, as the thickness increases the first mode becomes damped and the second mode then dominates. In this case the increase in frequency at constant  $d$  giving the change of  $z_1 \rightarrow z_2$  would produce the transition indicated by c). Similarly to b) this would result in a lower mass sensitivity than at the initial, lower, frequency. In contrast, the change indicated by d) which uses a change of  $z_2 \rightarrow z_3$  (and a change of mode) due to increasing the frequency whilst retaining the same thickness guiding layer results in an increased sensitivity. In fact, beginning with a Love wave with a wave-guiding layer optimised so that its operating point is at the maximum slope of the first Love wave mode, the maximum change in mass sensitivity obtainable by increasing the operating frequency is by changing modes. Thus, for the data in Figure 2, an increase in frequency by a factor of 3.04 gives an increase in the peak sensitivity of 1.51 rather than by a factor of 3.04 which might be imagined from the explicit frequency pre-factor evident in Eq. (9). This is a consequence of the lower maximum slope available from the second Love wave mode compared to the first. Similarly, frequency hopping a given optimised device by a factor of 5.08 will move the peak sensitivity of the first mode to the peak sensitivity of the third mode and give an increase in sensitivity of only 1.77.

### 3.3 OPTIMISED HIGH FREQUENCY DEVICES

A second type of frequency change is to construct two Love wave devices operating at two different frequencies and then optimise the guiding layer thickness of each so that maximum mass sensitivity is obtained for the first Love wave mode. In this manner, the operating point on the dispersion curve does not change between the two devices and the mass sensitivity from Eq. (9) is then predicted to increase linearly with frequency. Thus we have a result analogous to that of a QCM sensor - the frequency dependence of the sensitivity function  $S_m$  is proportional to the frequency for a uniform layer of mass provided the wave-guiding thickness is chosen for the optimum operating point and the same mode. This analogy can also be rigorously extended to Love wave sensors operating in liquids, i.e. the frequency dependence of the sensitivity function  $S_m$  is proportional to the square root of frequency for a Newtonian liquid provided the wave-guiding thickness is chosen for the optimum operating point and the same mode.

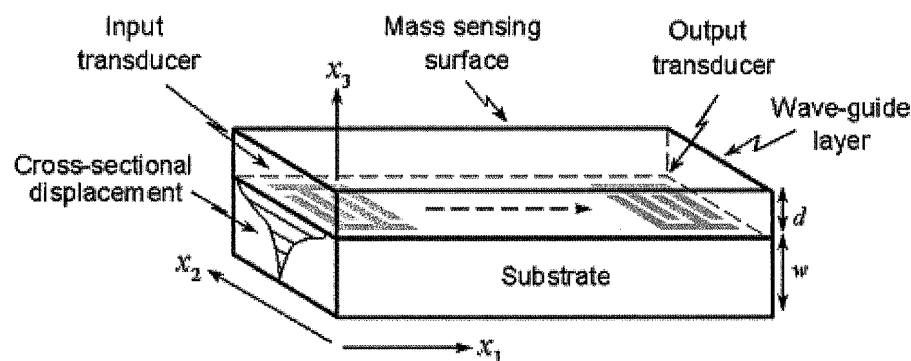
#### 4. CONCLUSION

This paper has outlined theoretical advances in understanding the use of Love waves for sensing. A model has been developed which gives a unified treatment of two hitherto separate types of sensor, Love wave and SH-APM. The idea of a SH-APM has been extended to a new concept of a layer guided SH-APM sensor. The model shows that higher order Love waves on finite thickness substrates can be regarded as continuations of these layer guided SH-APMs. Moreover, the use of a wave-guiding layer on a SH-APM device suggests significantly enhanced mass sensitivity may be possible whilst retaining the advantage of operating the device with transducers fabricated on the opposing face to that with the guiding layer exposed to liquid. The frequency dependence of the mass sensitivity of traditional Love wave sensors has also been examined. The relationship between the slope of the dispersion curve and the mass sensitivity has been made explicit and general rules for operating higher frequency sensors obtained. A difference in sensitivity obtainable by increasing the frequency of a given device and by optimising the wave-guiding layer of a higher frequency device has been identified. It has been shown that the peak sensitivity of a given Love wave mode obtained by optimising the wave-guiding layer thickness increases linearly with frequency when sensing uniform mass layers.

#### Acknowledgements

The authors gratefully acknowledge the BBSRC for financial support under research grant 301/E11140. We also acknowledge F. Martin for help in formulating the ideas in this work.

(a)



(b)

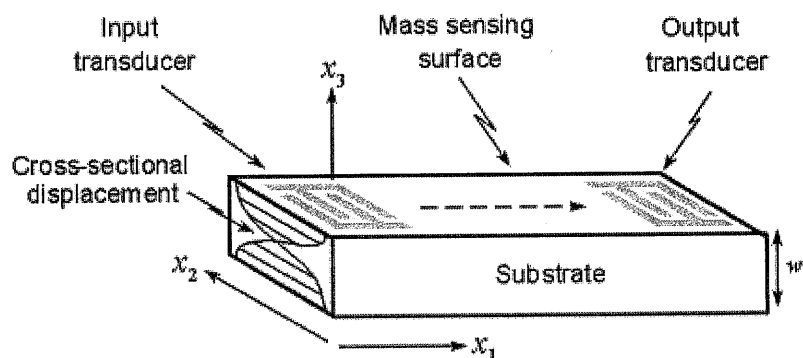


Figure 1. (a) Love wave and (b) SH-APM sensor configurations. In each case mode propagation is parallel to the  $x_1$ -axis with displacements in the  $x_2$  direction. The Love wave decays with depth whilst the SH-APM uses a substrate resonance; the lowest order mode is indicated schematically in both cases.

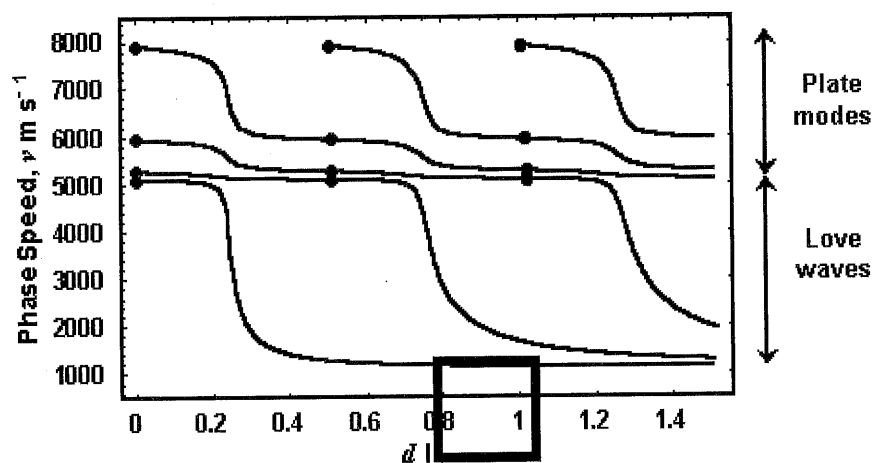


Figure 2. Phase speed calculated numerically from the dispersion equation for a two-layer system of substrate and wave-guiding layer. The points are values known from analytical results. Curves with  $v < v_s$  correspond to Love waves and curves with  $v > v_s$  correspond to layer guided SH-APMs.

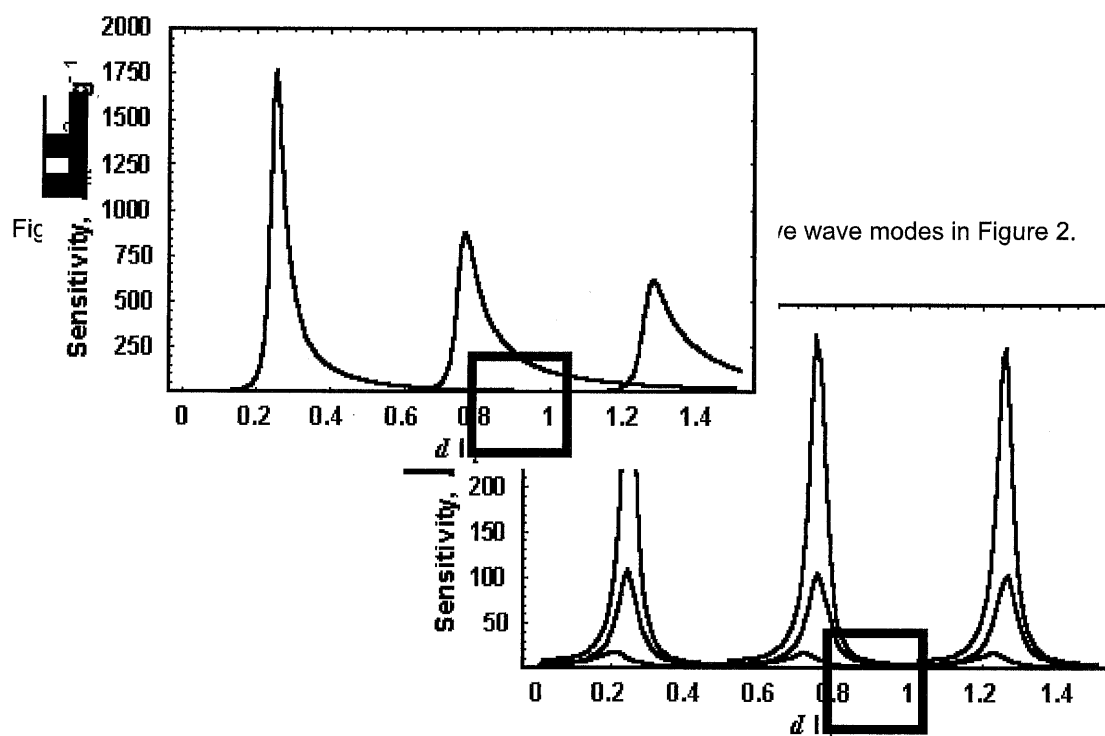


Figure 4. Modulus of mass sensitivity,  $|S_m|$ , for the layer guided SH-APMs associated with the three Love wave modes in Figure 3.

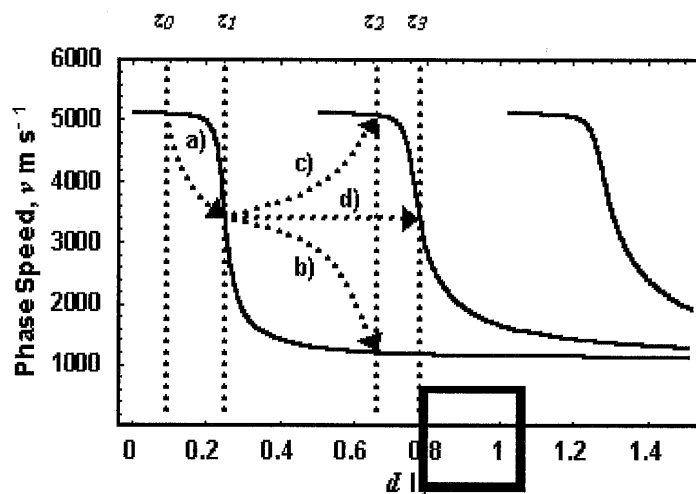


Figure 5. Possible changes of Love wave operating points due to change of frequency.